Differential Epidermal Growth Factor Receptor Signaling Regulates Anchorage-Independent Growth by Modulation of the PI3K/AKT Pathway

Joseph O. Humtsoe and **Randall H. Kramer**

Department of Cell and Tissue Biology, University of California San Francisco, San Francisco, California

Abstract

Tumor cells are capable of surviving loss of nutrients and anchorage in hostile microenvironments. Under these conditions adapting to specific signaling pathways may shift the balance between growth and cellular dormancy. Here we report a mechanism by which EGFR differentially modulates the PI3K/AKT pathway in cellular stress conditions. When carcinoma cells were cultured as multicellular aggregates (MCA), cyclin D1 was induced through a serum-dependent EGFR activating pathway, triggering cell proliferation. The expression of cyclin D1 required both EGFR-mediated ERK and AKT activation. In serum-starved MCAs, EGFR activation was associated with active ERK1/2 but not AKT and failed to induce cyclin D1. Analysis revealed that, under serum-starved conditions, EGFR-Y1086 residue was poorly autophosphorylated and this correlated with failure to phosphorylate Gab1. Accordingly, the EGFR activation failed to induce EGFR/PI3K complex formation or AKT activation, preventing cyclin D1 induction. Furthermore, we show that in serum-starved MCA, expression of constitutively active AKT re-established cyclin D1 expression and induced proliferation in an EGFR-dependent manner. Thus, modulation of the PI3K/AKT pathway by context-dependent EGFR signaling may regulate tumor cell growth and dormancy.

Keywords

Cell-cell adhesion; EGFR; PI3K/AKT

The coordinated signaling generated through extracellular matrix (ECM) adhesion and growth factors are essential for normal epithelial cell survival, growth and proliferation (Cabodi et al., 2004; Miranti and Brugge, 2002). Depriving normal adherent cells from ECM anchorage can lead to cellular stress that eventually may initiate programmed cell death or anoikis (Frisch and Screaton, 2001; Gilmore, 2005). However, during tumor progression, malignant cells are generally capable of overcoming the lack of proper cellular adhesion to the ECM and nutrient deprivation. Under these microenvironmental stress conditions, cells

---

Corresponding Author: Randall H. Kramer, PhD, Department of Cell and Tissue Biology, UCSF, 521 Parnassus Avenue, Room C-640, San Francisco, CA- 94143-0640, Tel: 415-476-3275; Fax: 415-476-1499, randall.kramer@ucsf.edu.

must adapt specific signaling pathways that promote their survival, growth and tumor dormancy (Aguirre-Ghiso, 2007; Alt-Holland et al., 2005; Ranganathan et al., 2006). The cellular mechanisms controlling these pathways remain complex and poorly understood.

Cell spheroids or multicellular aggregates (MCA) represent an anchorage-independent culture model designed to recapitulate the in vivo three-dimensional solid tumors (Bates et al., 2000). The formation of these aggregates is dependent on the engagement of cellular adhesion receptors, such as the cadherins. From this 3-D model system, it is strongly evident that the extensive intercellular adhesions can mediate signals to circumvent ECM-dependency and promote survival and growth regulating response (Bates et al., 2000; Santini et al., 2000). Insights gained from these studies provide an additional facet in understanding the adverse nature of the tumor microenvironment and holds a promising model system for therapeutic drug development (Alt-Holland et al., 2005; Friedrich et al., 2007).

Previously we showed that ligand-independent epidermal growth factor receptor (EGFR) activation acts as a survival signal in squamous cell carcinoma MCAs (Kantak and Kramer, 1998; Shen and Kramer, 2004). This work demonstrates that EGFR-mediated survival effects were primarily through activation of ERK, but not AKT. EGFR is one of the receptor tyrosine kinases that can trigger phosphatidylinositol 3′-kinase (PI3K) -mediated AKT activation (Engelman, 2009; Manning and Cantley, 2007). Despite activated EGFR, phospho-AKT was not detected; nor did specific chemical inhibitors of AKT induce cell death in MCA (Shen and Kramer, 2004). This phenomenon may represent an example of context-dependent EGFR-mediated PI3K/AKT signaling. Defining the underlying cellular events involved here may provide insights on the mechanism by which EGFR modulates tumor cell survival and growth in the adverse and dynamic microenvironment encountered during tumor progression.

In the current report, we have examined the mechanism of ligand-independent EGFR signaling using the squamous cell carcinoma 3-D model. To mimic the physiologically relevant growth promoting or restricting environment, these studies were performed in serum-stimulated and serum-starved conditions, respectively. We found that EGFR signaling in serum-starved MCA failed to support cyclin D1 protein expression and cell proliferation. This was in contrast to serum-stimulated MCAs where cyclin D1 expression was positively regulated through EGFR-mediated ERK and AKT activation. Analysis of EGFR activation in serum-starved MCA as well as use of ILR-EGFR-chimera revealed that depending on the mode of activation, EGFR can act differentially in its ability to couple the Gab1/PI3K/AKT signaling module. Thus, we hypothesize that by modulating the PI3K/AKT pathway; microenvironment-dependent EGFR signaling may regulate cyclin D1 expression and the cellular proliferative response.

MATERIALS AND METHODS

Reagents and cell culture conditions

The following antibodies were obtained as follows: PI3K-p85 (Millipore, Inc.); EGFR, E-cadherin, Gab1, cyclin D1 (Santa Cruz Biotech., CA); p-ERK1/2, ERK1/2, p-AKT, AKT

and Grb2, and inhibitors U0126 and LY294002 (Cell Signaling Technology, Inc.); activated-EGFR, Shc, pY20 and tubulin (BD Biosciences); phospho-specific EGFR antibodies (Biosource,.); Flag-M2 (Stratagene Inc.). AG1478 and PD168393 were purchased from Calbiochem (San Diego, CA). Recombinant human E-cadherin/Fc chimera (hE-Cad/Fc) was purchased from R&D systems, Inc.

Human squamous carcinoma cells (HSC-3, HSC-2, MOK-101, SCC-4 and Ca9–22) as previously described (Chen et al., 2004; Matsumoto et al., 1994) and HEK293 were maintained in Dulbecco's Modified Eagle Media (DMEM) containing 10% fetal bovine serum (FBS) (Invitrogen, Inc, CA). Methods for generating multicellular aggregates (MCA) and single cell suspension cultures on poly-HEMA (Sigma, St. Louis, MO) established previously were followed (Kantak and Kramer, 1998; Shen and Kramer, 2004).

For cell proliferation assay, serum-starved HSC-3 cells were subjected to MCAs for 24 h in DMEM containing 50 μM 5-bromo-2-deoxyuridine (Sigma). MCAs were collected, dissociated to single cells by trypsinization, then washed and allowed to attach on poly-L-Lysine coated coverslips and processed for staining as previously described (Humtsoe et al., 2003).

EGFR-chimera constructs

Full length EGFR and EGFR-chimeras were generated using pXf-EGFR (A. Wells, UP, PA) and interleukin 2 receptor alpha (ILR) (K. Wary, UIC, IL) cDNA as templates. The ILR-wt, ILR- JD and ILR- KD were generated by two-step PCR reactions using primers obtained from IDT (Coralville, IA). The constructs were then inserted into Flag-epitope expression vector pCMV-Tag 4 (Stratagene).

Immunoblotting and immunoprecipitation

Cell lysates were prepared in cell extraction buffer as described previously (Humtsoe et al., 2003) and quantified using BCA Protein Assay (Pierce Inc). For immunoprecipitation, 0.5–1.5 mg of total cell lysates was used. The immunocomplexes or total cell lysates were resolved by SDS-PAGE, transferred to Immobilon PVDF membranes (Millipore, Inc) and immunoblotted and detected as previously described (Humtsoe et al., 2003).

hE-Cad/Fc coated beads assay

Polystyrene beads (15 μm diameter) for coating were carried out in borate buffer per instructions (Polysciences, Inc.). After pre-coating overnight with nitrocellulose (Goodwin et al., 2003), beads were washed and re-coated with hE-Cad/Fc (50 μg/ml) or BSA (10 mg/ml). Beads were suspended in PBS containing 10 mg/ml BSA, 0.02% sodium azide and 5% glycerol, and stored at 4°C until use. For hE-Cad/Fc mediated EGFR activation in MCA assay, serum-starved HSC3 cells were detached and incubated with the beads on poly-HEMA plates. Cell aggregates with bound beads were collected, lysed and processed for immunoblot analysis.

Co-expression culture assay

Normal HEK293 or HEK293 cells stably transfected with EGFR alone or double-transfected with EGFR and the E-cadherin construct Ec1M (Chitaev and Troyanovsky, 1998), were used in this assay. Cells were seeded into six well culture plates in DMEM (no serum) at high density (4×10^6 cells/ml) to promote rapid and efficient cell-cell contacts. At different time points, cells were harvested and lysates were prepared for Western blot analysis.

RNA Interference

The ON-TARGETplus SMARTpool siRNA targeting the EGFR and Gab1, as well the non-targeting control siRNA were purchased from Dharmacon, Thermo Scientific (Lafayette, CO). The Lipofectamine RNAiMAX for the siRNA transfection was purchased from Invitrogen Corporation (Carlsbad, CA). Monolayer HSC-3 cells were transiently transfected in serum-free media. After 24 hr cells were detached and subjected to MCA formation for another 20–24 hr before analysis.

RESULTS

Serum starvation suppresses cyclin D1 expression and proliferation in anchorage-independent MCA

To study cellular growth mechanisms under microenvironmental stress conditions we utilized the MCA model (Kantak and Kramer, 1998; Shen and Kramer, 2004) and generated MCAs in serum-stimulated and starved conditions for 24 h. Figure 1A shows the presence of strong cyclin D1 protein in serum-stimulated MCA, but only a low level in serum-deprived MCA. The expression of cyclin D1 did not show a significant serum dependency in monolayer culture. Under identical conditions, the BrdU uptake in serum-starved MCAs was about 4% whereas serum-stimulation showed increased labeling of approximately 19% (Figure 1B). However, we did not detect any significant difference in cell viability or the ability to adhere and scatter on tissue culture plates between the serum-stimulated and serum-starved MCAs (Supplemental Figure 1A–B). Together these results show that serum-deprivation suppresses cyclin D1 expression and proliferation in MCA.

Serum-deprived EGFR activation in MCA is not sufficient for cyclin D1 expression and proliferation

To investigate the possible role of EGFR activation in modulating cell growth under stress-induced conditions, serum-deprived MCAs were analyzed for EGFR phosphorylation. EGFR activation was evident as cells progressed from loose to more compact MCAs, even in the absence of serum-factors (Figure 1C–D). However, the level of cyclin D1 protein expression gradually decreased, showing a significant reduction by 9 and 24 h. Concomitantly, there was a dramatic increase in p27 expression at 24 h. As expected adherent monolayer cells continued to maintain high cyclin D1 but low p27 protein expression under serum-starved conditions. The observed loss of cyclin D1 protein expression in serum-starved MCAs after 24 h was similar to that of cells incubated as a single cell (S) suspension (Figure 1E), which lack proliferation capabilities and eventually undergo anoikis; (Kantak and Kramer, 1998). But unlike cells in suspension, MCA

displayed strong ERK phosphorylation that is consistent with our previous report (Shen and Kramer, 2004). However, the presence of serum did not appear to further enhance the ERK phosphorylation. The presence of constitutively activated ERK in MCAs appears to over-ride the serum-induced ERK activity. In contrast, only weak AKT phosphorylation was observed in MCAs and single cell suspension. Since cyclin D1, an EGFR target gene, is essential for cell-cycle progression, it implies that in the absence of serum and ECM attachment, a likely ligand-independent EGFR signaling is not sufficient to promote robust cell proliferation.

To directly test ligand-independent EGFR signaling, we generated a EGFR-chimera lacking a ligand-binding region that exhibits constitutive kinase activity (Bernard et al., 1987) (Figure 2A). Since HSC-3 cells express high levels of endogenous EGFR, we used HEK293 cells that express undetectable levels of endogenous EGFR for the transfection studies. These well-characterized cells contain protein molecules necessary for EGFR signaling (Cai et al., 2006; Schmidt et al., 2003). Analysis confirmed efficient cell surface expression of the ILR-EGFR-chimera proteins (Supplemental Figure 2A). The ILR-wt chimera displayed strong phosphorylation activity resulting in ERK1/2 but not AKT phosphorylation (Figure 2B). The ILR- JD and ILR- KD similar to the vector-control did not exhibit any phosphorylation nor did it transduce downstream ERK1/2 phosphorylation. Confirming the intrinsic kinase function of ILR-wt, an EGFR inhibitor (AG1478), but not a Src-inhibitor (SU6656) blocked phosphorylation activity of the chimera and ERK1/2 in a dose-dependent manner (Supplemental Figure 2B; data not shown). Subsequently, we used ILR-wt as a ligand-independent active EGFR and the ILR- JD as an inactive chimera control.

We next tested the ILR-wt construct on the expression of cyclin D1. The full length EGFR (FL-wt) transfected HEK293 cells stimulated with EGF, as well as normal cells grown in presence of serum, effectively induced the expression of cyclin D1 (Figure 2C). However, cyclin D1 protein induction was lacking in the ILR-wt expressing cells despite the strong phosphorylation activity. Cyclin D1 expression was also not detected in the unstimulated, vector-control or ILR- JD cells. Stimulation of FL-wt HEK293 cells with EGF modestly increased the rate of DNA synthesis, while the ILR-wt did not support HEK293 cell proliferation. However, after being subjected to 24 h suspension-induced apoptosis, the ILR-wt expressing cells produced about 75% cell survival compared to approximately 30% in the vector-control and ILR- JD (Supplemental Figure 2C–D). These results support the observations that serum-deprived EGFR activation in MCAs, likely ligand-independent, generates an effective survival signal without induction of cyclin D1 or cell proliferation.

Serum-dependent cyclin D1 expression in MCA requires EGFR signaling

To study the role of EGFR signaling in regulating cyclin D1 expression in the microenvironment of cell aggregates, we used two potent EGFR inhibitors, PD168393 and AG1478 (Onishi et al., 2008). We initially evaluated the time course of serum-stimulation required for cyclin D1 expression in pre-formed MCAs. Cyclin D1 induction was evident at 3 h and expression reached a plateau at 6 h (Figure 3A). Whereas EGFR and ERK1/2 phosphorylation was readily detected in MCAs with or without serum, neither p-AKT activity nor cyclin D1 expression was evident in the serum-free MCAs (Figure 3B).

However, serum-stimulation induced AKT phosphorylation and showed robust induction of cyclin D1 protein (Figure 3B,g). Inhibition of EGFR activity in 6 h MCA with either 1 or 10 μM PD168393 or AG1478 blocked serum-induced AKT and ERK1/2 phosphorylation, and correlated with cyclin D1 reduction. Treatment with U0126 and LY294002 also blocked ERK1/2 and AKT phosphorylation, respectively, and led to inhibition of cyclin D1 expression (not shown). Serum-stimulation also increased the cyclin D1 induction in a set of HNSCC cell lines, SCC-4, MOK-101, Ca9-22 and HSC-2 cells, although with varying efficiency. In addition, the levels of cyclin D1 expression were lowered with EGFR inhibition (Supplemental Figure 3AB). To confirm the specificity of EGFR, a siRNA mediated knockdown of EGFR was employed that strongly inhibited the serum induced-phosphorylation of AKT and ERK in MCAs (Figure 3C). Concomitantly, there was decrease in the serum stimulated induction of cyclin D1 protein. These results imply that serum-induced cyclin D1 expression in anchorage independent MCA is mediated primarily through EGFR, which signals upstream of PI3K and MAPK activation.

Serum dependent cyclin D1 expression in MCA is associated with Y1086 EGFR autophosphorylation

Activated EGFR in serum-starved MCA does not support cyclin D1 expression (Figure 1). However, serum-stimulated cyclin-D1 expression is mediated through EGFR activation (Figure 3). To understand the mechanism, we set out to evaluate the EGFR autophosphorylation activity during serum deprived formation of MCA. Using a panel of five phospho specific EGFR antibodies, we observed low level phosphorylation of EGFR-tyrosine residues during the initial 3 h of culture (Figure 4A). However, at 6 and 24 h enhanced phosphorylation was detected at tyrosine residues Y845, Y1068, Y1148 and Y1173 that correlated with the progressed formation of compacted MCAs. Surprisingly, residue Y1086 showed minimal phosphorylation under the same conditions. Monolayer cell controls showed that EGF readily induced strong phosphorylation at all tyrosine sites including residue Y1086. This confirmed the specificity of the antibodies, which have also been successfully used by others (Moro et al., 2002). To rule out a defective Y1086 residue in the aggregates, MCAs were stimulated with EGF for varying time periods (Figure 4B). EGF treatment showed robust induction of phosphorylation at residue Y1086 at all time points. Next, we tested whether inefficient EGFR-Y1086 autophosphorylation was associated with reduced cyclin-D1 levels in serum-starved MCAs. Immunoblotting revealed that residues Y845, Y1068, Y1148 and Y1173 were readily phosphorylated in both serum-deprived and serum-stimulated MCAs (Figure 4C). However, residue Y1086 phosphorylation and cyclin D1 expression was only weakly detectable in serum-deprived MCAs. Exposure to low- and moderate-serum (1 and 10 % FBS) appeared to induce the phosphorylated level of Y1086, and this correlated with the enhanced cyclin D1 expression. As expected, PD168393 and AG1478 effectively blocked the EGFR phosphorylation pattern and cyclin D1 induction. Though additional studies are needed to further define the precise mechanism by which serum-factors induce EGFR activation, our results show that in serum-deprived MCA the EGFR activation produces an inefficient receptor autophosphorylation pattern.

Ligand-independent EGFR activation mediates selective tyrosine autophosphorylation

To further evaluate the unique ligand-independent EGFR autophosphorylation pattern observed above, we employed a series of assays using HSC-3 and HEK293 cells. Initially, the ability of hE-cad/Fc beads to induce E-cadherin recruitment on HSC-3 monolayer cells and cluster with aggregating cells on poly-HEMA substrate was evaluated (Supplemental Figure 4A–B). Since cell aggregation progressed between 3 and 6 h, we incubated HSC-3 cells with hE-cad/Fc- or BSA-coated beads for 4 h prior to analysis. hE-cad/Fc beads induced enhanced EGFR phosphorylation as compared to control BSA-coated beads but relatively at lower level compared to EGF-treated cells (Figure 5A). Cells treated with hE-cad/Fc beads displayed phosphorylation activity at residue Y845, Y1148 and Y1173, but Y1086-autophosphorylation remained at background levels (Figure 5B).

Furthermore, in a Ca^{2+}-switch assay we observed the phosphorylation at Y845, Y1068, Y1148 and Y1173 as cells formed Ca^{2+}-induced cell-cell contact (Figure 5C). However, Y1086 phosphorylation was not detected even after prolong x-ray film exposure. Yet, EGF treatment induced strong autophosphorylation at all residues including Y1086.

HEK293 cells co-expressing EGFR and E-cadherin displayed EGFR phosphorylation but not in cells expressing EGFR alone upon 30 min seeding on culture dish (Supplemental Figure 4C). On further analysis, we observed that residues Y845, Y1068, Y1148 and Y1173 were readily autophosphorylated, while residue Y1086 phosphorylation was barely detectable (Figure 5D). The HEK293-EGFR cells treated with EGF showed strong Y1086 phosphorylation.

Next, we examined the autophosphorylation status in the ILR-wt chimera. Phosphorylation at residues Y845, Y1068, Y1143 and Y1173 were readily detected in the ILR-wt and EGF-treated FL-wt expressing cells (Figure 5E, a–b, d–e). However, autophosphorylation at residue Y1086 of constitutive active ILR-wt was consistently weak or absent (Figure 5E, c). Taken together, these results support the observations made from the MCA experiments that ligand-independent EGFR activation induces unique autophosphorylation pattern.

Ligand-independent EGFR activation fails to recruit Gab1/PI3K/AKT signaling complex

The results thus far indicate that MCAs require efficient and promiscuous EGFR autophosphorylation, with concurrent AKT and ERK activation to induce cyclin D1 expression under anchorage-independent conditions. This suggested a mechanistic relationship between inefficient EGFR autophosphorylation and the failure to induce AKT activation. We found that in EGF or serum-stimulated MCAs, EGFR co-immunoprecipitated with the PI3K regulatory p85 subunit; and this association correlated with the phosphorylation of EGFR-Y1086 and AKT (Figure 6A). In contrast, under serum-starved conditions neither p85 immunoreactivity nor AKT activation was detected. Interestingly, EGFR co-immunoprecipitated Shc and Grb2 independent of serum stimulation. This complex formation was however, at lower levels when compared with EGF induction. Expectedly, PD168393 treatment inhibited serum-stimulated EGFR-Y1086 and AKT phosphorylation and reduced the association of Shc and Grb2 with EGFR. Similarly, HEK293 cells expressing FL-wt treated with EGF induced strong EGFR phosphorylation

and co-precipitated p85, Shc and Grb2. Interestingly, the ILR-wt chimera failed to associate with p85, as did the vector control and the inactive ILR- JD chimera (Figure 6B). However, ILR-wt was strongly phosphorylated and efficiently co-precipitated Shc and Grb2.

The adaptor protein Gab1 is phosphorylated during EGFR-mediated PI3K/AKT signaling (Holgado-Madruga et al., 1996; Mattoon et al., 2004). In HSC-3 MCA, Gab1 was tyrosine phosphorylated upon serum-stimulation with or without EGF treatment, and this effect was totally abolished by PD168393 (Figure 6C). Remarkably, there was no evidence of Gab1 phosphorylation activity from serum-starved MCAs, despite having EGFR in its active phosphorylated form. To further confirm this observation, we analyzed HEK293 cells expressing the ILR-wt. Whereas FL-wt EGFR cells stimulated with EGF induced strong Gab1 phosphorylation, the ILR-wt cells failed to do so and was similar to the vector, FL-wt (untreated) or ILR- JD cells (Figure 6D). To further confirm the specificity of EGFR activation on the Gab1 phosphorylation, a siRNA-mediated knockdown of EGFR was employed. The knockdown of EGFR protein strongly reduced the serum-induced phosphorylation of Gab1 in MCAs (Figure 6E). Next, to examine the role of Gab1 in the EGFR-mediated AKT activation, we used siRNA to knockdown Gab1. Reducing the Gab1 expression abolished the ability of EGFR to associate with p85 in serum-induced MCAs (Figure 6F). Analyses of the lysates show that Gab1 knockdown reduced the serum-induced AKT phosphorylation. Together, the above results clearly indicate that ligand-independent EGFR activation is not sufficient in recruiting p85 or Gab1 phosphorylation to mediate AKT signaling.

Constitutively active AKT rescues EGFR-dependent cyclin D1 expression and proliferation in serum-deprived MCA

Is the suppression of cyclin D1 expression and proliferation in serum-deprived MCA a consequence of ineffective AKT signaling? We tested whether reconstitution of active AKT would restore cyclin D1 protein expression and induce proliferation in HSC-3 cells expressing GFP-tagged AKT. Initially, the constitutively active-AKT1 (CA-AKT) expression and activity were confirmed by fluorescence microscopy and immunoblotting with phospho-AKT (Supplementary Figure 5A–B). In GFP or KD-AKT (kinase-dead) expressing MCAs, cyclin D1 expression was at basal levels but following serum-stimulation cyclin D1 were induced by over 2-fold (Figure 7A, GFP and KD-AKT compare lanes 1–2). As expected, inhibition of EGFR and MAPK activity blocked the serum-induced elevation of cyclin D1 expression (Figure 7A, GFP and KD-AKT, compare lane 3–4). In contrast, CA-AKT expression in MCA under serum-free conditions promoted cyclin-D1 expression to a level comparable to serum-stimulation (Figure 7A, CA-AKT, compare lanes 1–2). Interestingly, in cells expressing CA-AKT, inhibition of both EGFR and MAPK activity blocked serum-stimulated cyclin D1 protein expression. Immunoblotting indicates that the status of phosphorylated EGFR or ERK1/2 in MCA is not altered by CA-AKT expression, whether in the absence or presence of serum. The CA-AKT mediated cyclin D1 expression in absence of serum can also be suppressed by U0126 (Figure 7B). This indicate that MAPK and AKT signaling cooperates to modulate cyclin D1 expression in MCA. Since expression of KD-AKT showed no difference in cyclin D1 protein levels compared to control GFP, we next measured DNA synthesis in the GFP-control or CA-AKT expressing MCAs. Figure 7C

shows that CA-AKT potentiated BrdU incorporation by about three-fold over GFP-control expressing MCAs, even in serum-deprived conditions. In the CA-AKT expressing MCAs, the presence of serum did not further enhance the proliferative capability of the cells. However, inhibiting the EGFR function reverted the proliferative effect back to serum-free GFP-control levels. This parallels the cyclin D1 expression pattern indicating that activated EGFR/ERK and AKT are both essential in the control of cell proliferation in MCAs.

DISCUSSION

The importance of normal cell dependence on the ECM in linking cyclin D1 expression to cell cycle progression and growth in vitro is well documented (Miranti and Brugge, 2002; Walker and Assoian, 2005). In the absence of attachment to ECM substrates, growth factor-stimulated cells are unable to induce cyclin D1. Our study with HNSCC cells, cultured as anchorage-independent MCA show a serum-dependent cyclin D1 expression and proliferation. Notably, analysis of EGFR signaling in serum-stimulated and -starved MCA revealed that depending on the mode of activation, EGFR differentially modulate the Gab1/PI3K/AKT signaling pathway and regulate cyclin D1 expression and proliferation.

Previous work reported that formation of MCAs by HNSCC cells induces adhesion-mediated ligand-independent EGFR/ERK activation (Shen and Kramer, 2004). Indeed, in serum-deprived MCAs, EGFR/ERK was constitutively activated while AKT remained inactive. However, the presence of adhesion-mediated ligand-independent active EGFR and ERK1/2 was not sufficient to promote the cell proliferative response as suggested by the diminished cyclin D1 and increased p27 protein expressions. EGFR signaling through endocrine, autocrine and juxtacrine mechanism are known (Schneider and Wolf, 2009; Singh and Harris, 2005). For example, HB-EGF-mediated juxtacrine signaling is sufficient to trigger strong AKT activation (Singh et al., 2007). Though such mechanisms are possible, the EGFR activation in serum-deprived MCA was unable to trigger active AKT or promote cyclin D1 expression or proliferation.

Blocking EGFR function inhibits the expression of cyclin D1 and proliferation (Lenferink et al., 2001). It is also known that EGFR-mediated cell proliferation requires integrin-mediated cell adhesion to the ECM (Bill et al., 2004; Kuwada and Li, 2000). We found that in HNSCC cell aggregates, EGFR-mediated serum-dependent cyclin D1 expression. In this study, we focused on the HSC-3 cells since this HNSCC cell line, derived from a cervical lymph node metastasis of a tongue primary lesion, has been shown to retain both its in vivo tumorigenicity and metastatic potential in the nude mouse model, and has been extensively characterized for its in vitro and in vivo phenotype and responsiveness to EGFR and other growth factors (Bourguignon *et al.*, 2006; Kawano *et al.*, 2001; Nurmenniemi *et al.*, 2009; Onishi *et al.*, 2008). The results obtained in the current studies seem relevant to HNSCC since serum-stimulation enhanced EGFR-dependent cyclin D1 induction in a panel of four other well-characterized HNSCC cell lines. Other studies in anchorage-independent cultures, using MCF10A and Ewing tumor sarcoma cells have shown that AKT but not ERK signaling is essential in intercellular adhesion-mediated cyclin D1 expression and growth (Fournier et al., 2008; Kang et al., 2007; Lawlor et al., 2002). Our study in HNSCC cell

aggregates show that EGFR-dependent ERK and AKT activation are both important in that they act synergistically to regulate cyclin D1 expression.

What is the mechanism by which activated EGFR acts differentially under the two conditions (serum-stimulated versus serum-starved)? We identified EGFR-Y1086 as a unique residue inefficiently autophosphorylated in the serum-deprived cell aggregates. Cells that form cell aggregates do so by forming a complex 3-D network of intercellular adhesions. The role of E-cadherin in mediating these cell-cell interactions and transactivation of EGFR has been established (Pece and Gutkind, 2000; Shen and Kramer, 2004). Employing several approaches involving E-cadherin and EGFR-chimera constructs, we were able to confirm the unique pattern of ligand-independent EGFR autophosphorylation.

EGFR-Y1086 is one of the major tyrosine residues located at the cytoplasmic region that is readily phosphorylated during EGFR kinase activation. This, in turn, can mediate downstream signaling events by binding with molecules such as Grb2, Shc, Gab1, STAT3 and c-Abl (Jorissen et al., 2003; Thelemann et al., 2005). In line with our observation of persistence ERK activity, ligand-independent EGFR activation associated with the signaling adaptor proteins, Grb2 and Shc. EGFR is known to associate with the PI3K/p85 regulator subunit and induce PI3K-mediated AKT activation (Hu et al., 1992). However, our findings clearly suggest that though competent in Grb2 and Shc binding and ERK activation, ligand-independent EGFR activation is unable to complex with the PI3K/AKT signaling module.

Specificity of signaling by receptor tyrosine kinases depends on interaction with specific substrates as well as with substrates shared by other signaling-competent receptors. For example, Gab1 is a docking protein involved in the downstream signaling of many types of tyrosine receptor kinases, including EGFR (Holgado-Madruga et al., 1996; Weidner et al., 1996). Upon EGFR activation, Gab1 undergo tyrosine phosphorylation and potentiate EGF-mediated activation of the PI3K/AKT pathway (LeVea *et al.*, 2004; Mattoon *et al.*, 2004). To our knowledge, we show here for the first time that ligand-independent EGFR activation is unable to phosphorylate Gab1. Since residue Y1068 and Y1086 of EGFR have been shown to be important for EGFR/Gab1 association (Rodrigues et al., 2000), this finding highlights the significance of inefficient EGFR-Y1086 autophosphorylation. It warrants future work to specifically examine mutated EGFR-Y1086F and its various signaling responses. Nevertheless, it is conceivable that phosphorylation at both Y1068 and Y1086 residues is critical and essential for efficient EGFR/Gab1 associations and subsequent Gab1 phosphorylation. In serum-deprived MCAs, the lack of efficient Gab1 phosphorylation may uncouple the EGFR/PI3K/AKT activation, thereby fail to promote cyclin D1 expression and proliferation. This possibility is likely because the expression of constitutively active AKT was able to by-pass inefficient EGFR activation and permit cyclin D1 induction and proliferation.

EGFR mediates PI3K/AKT signaling and regulates VEGF expression in hypoxic conditions (Jiang et al., 2001; Pore et al., 2006). Similarly, loss of EGFR function has been suggested to contribute during stress signaling induction, which in turn might influence tumor dormancy (Aguirre-Ghiso, 2007). Under serum-deprivation, tumor cell-derived factors like

Clusterin can modulate the PI3K/AKT pathway to determine growth and dormancy (Jo et al., 2008). Thus, under unfavorable growth conditions, the ability of EGFR to regulate PI3K/AKT activation may bear important physiological implications. We hypothesize that during limited availability of nutrients/serum (e.g., due to poor vascularization), tumor islands of compact cell aggregates utilize differential EGFR signaling to uncouple the PI3K/AKT pathway yet still maintaining the ERK survival pathway. This may in turn act as an alternate mechanism to prevent cells from entering active cell-cycle progression and promote growth arrest. The presence of dormant tumor cell clusters in non-permissive microenvironment may be resistant to chemotherapy or irradiation and present significant challenges to treatment of disseminated disease. Thus, understanding such microenvironmental-derived survival pathways may suggest novel therapeutic approaches that could target dormant tumor cell in micrometastases.

Supplementary Material

Refer to Web version on PubMed Central for supplementary material.

Acknowledgments

References

Aguirre-Ghiso JA. Models, mechanisms and clinical evidence for cancer dormancy. Nat Rev Cancer. 2007; 7:834–46. [PubMed: 17957189]

Alt-Holland A, Zhang W, Margulis A, Garlick JA. Microenvironmental control of premalignant disease: the role of intercellular adhesion in the progression of squamous cell carcinoma. Semin Cancer Biol. 2005; 15:84–96. [PubMed: 15652453]

Bates RC, Edwards NS, Yates JD. Spheroids and cell survival. Crit Rev Oncol Hematol. 2000; 36:61–74. [PubMed: 11033297]

Bernard O, Fazekas de St Groth B, Ullrich A, Green W, Schlessinger J. High-affinity interleukin 2 binding by an oncogenic hybrid interleukin 2-epidermal growth factor receptor molecule. Proc Natl Acad Sci U S A. 1987; 84:2125–9. [PubMed: 3104909]

Bill HM, Knudsen B, Moores SL, Muthuswamy SK, Rao VR, Brugge JS, et al. Epidermal growth factor receptor-dependent regulation of integrin-mediated signaling and cell cycle entry in epithelial cells. Mol Cell Biol. 2004; 24:8586–99. [PubMed: 15367678]

Bourguignon LY, Gilad E, Brightman A, Diedrich F, Singleton P. Hyaluronan-CD44 interaction with leukemia-associated RhoGEF and epidermal growth factor receptor promotes Rho/Ras co-activation, phospholipase C epsilon-Ca2+ signaling, and cytoskeleton modification in head and neck squamous cell carcinoma cells. J Biol Chem. 2006; 281:14026–40. [PubMed: 16565089]

Cabodi S, Moro L, Bergatto E, Boeri Erba E, Di Stefano P, Turco E, et al. Integrin regulation of epidermal growth factor (EGF) receptor and of EGF-dependent responses. Biochem Soc Trans. 2004; 32:438–42. [PubMed: 15157155]

Cai W, He JC, Zhu L, Lu C, Vlassara H. Advanced glycation end product (AGE) receptor 1 suppresses cell oxidant stress and activation signaling via EGF receptor. Proc Natl Acad Sci U S A. 2006; 103:13801–6. [PubMed: 16954185]

Chen Q, Lipkina G, Song Q, Kramer RH. Promoter methylation regulates cadherin switching in squamous cell carcinoma. Biochem Biophys Res Commun. 2004; 315:850–6. [PubMed: 14985090]

Chitaev NA, Troyanovsky SM. Adhesive but not lateral E-cadherin complexes require calcium and catenins for their formation. J Cell Biol. 1998; 142:837–46. [PubMed: 9700170]

Engelman JA. Targeting PI3K signalling in cancer: opportunities, challenges and limitations. Nat Rev Cancer. 2009; 9:550–62. [PubMed: 19629070]

Fournier AK, Campbell LE, Castagnino P, Liu WF, Chung BM, Weaver VM, et al. Rac-dependent cyclin D1 gene expression regulated by cadherin- and integrin-mediated adhesion. J Cell Sci. 2008; 121:226–33. [PubMed: 18187454]

Friedrich J, Ebner R, Kunz-Schughart LA. Experimental anti-tumor therapy in 3-D: spheroids--old hat or new challenge? Int J Radiat Biol. 2007; 83:849–71. [PubMed: 18058370]

Frisch SM, Screaton RA. Anoikis mechanisms. Curr Opin Cell Biol. 2001; 13:555–62. [PubMed: 11544023]

Gilmore AP. Anoikis. Cell Death Differ. 2005; 12(Suppl 2):1473–7. [PubMed: 16247493]

Goodwin M, Kovacs EM, Thoreson MA, Reynolds AB, Yap AS. Minimal mutation of the cytoplasmic tail inhibits the ability of E-cadherin to activate Rac but not phosphatidylinositol 3-kinase: direct evidence of a role for cadherin-activated Rac signaling in adhesion and contact formation. J Biol Chem. 2003; 278:20533–9. [PubMed: 12672818]

Holgado-Madruga M, Emlet DR, Moscatello DK, Godwin AK, Wong AJ. A Grb2-associated docking protein in EGF- and insulin-receptor signalling. Nature. 1996; 379:560–4. [PubMed: 8596638]

Hu P, Margolis B, Skolnik EY, Lammers R, Ullrich A, Schlessinger J. Interaction of phosphatidylinositol 3-kinase-associated p85 with epidermal growth factor and platelet-derived growth factor receptors. Mol Cell Biol. 1992; 12:981–90. [PubMed: 1372091]

Humtsoe JO, Feng S, Thakker GD, Yang J, Hong J, Wary KK. Regulation of cell-cell interactions by phosphatidic acid phosphatase 2b/VCIP. Embo J. 2003; 22:1539–54. [PubMed: 12660161]

Jiang BH, Jiang G, Zheng JZ, Lu Z, Hunter T, Vogt PK. Phosphatidylinositol 3-kinase signaling controls levels of hypoxia-inducible factor 1. Cell Growth Differ. 2001; 12:363–9. [PubMed: 11457733]

Jo H, Jia Y, Subramanian KK, Hattori H, Luo HR. Cancer Cell-Derived Clusterin Modulates the PI3K-AKT Pathway through Attenuation of IGF-1 during Serum Deprivation. Mol Cell Biol. 2008

Jorissen RN, Walker F, Pouliot N, Garrett TP, Ward CW, Burgess AW. Epidermal growth factor receptor: mechanisms of activation and signalling. Exp Cell Res. 2003; 284:31–53. [PubMed: 12648464]

Kang HG, Jenabi JM, Zhang J, Keshelava N, Shimada H, May WA, et al. E-cadherin cell-cell adhesion in Ewing tumor cells mediates suppression of anoikis through activation of the ErbB4 tyrosine kinase. Cancer Res. 2007; 67:3094–105. [PubMed: 17409416]

Kantak SS, Kramer RH. E-cadherin regulates anchorage-independent growth and survival in oral squamous cell carcinoma cells. J Biol Chem. 1998; 273:16953–61. [PubMed: 9642258]

Kawano K, Kantak SS, Murai M, Yao CC, Kramer RH. Integrin alpha3beta1 engagement disrupts intercellular adhesion. Exp Cell Res. 2001; 262:180–96. [PubMed: 11139342]

Kuwada SK, Li X. Integrin alpha5/beta1 mediates fibronectin-dependent epithelial cell proliferation through epidermal growth factor receptor activation. Mol Biol Cell. 2000; 11:2485–96. [PubMed: 10888683]

Lawlor ER, Scheel C, Irving J, Sorensen PH. Anchorage-independent multi-cellular spheroids as an in vitro model of growth signaling in Ewing tumors. Oncogene. 2002; 21:307–18. [PubMed: 11803474]

Lenferink AE, Busse D, Flanagan WM, Yakes FM, Arteaga CL. ErbB2/neu kinase modulates cellular p27(Kip1) and cyclin D1 through multiple signaling pathways. Cancer Res. 2001; 61:6583–91. [PubMed: 11522658]

LeVea CM, Reeder JE, Mooney RA. EGF-dependent cell cycle progression is controlled by density-dependent regulation of Akt activation. Exp Cell Res. 2004; 297:272–84. [PubMed: 15194442]

Manning BD, Cantley LC. AKT/PKB signaling: navigating downstream. Cell. 2007; 129:1261–74. [PubMed: 17604717]

Matsumoto K, Matsumoto K, Nakamura T, Kramer RH. Hepatocyte growth factor/scatter factor induces tyrosine phosphorylation of focal adhesion kinase (p125FAK) and promotes migration and

invasion by oral squamous cell carcinoma cells. J Biol Chem. 1994; 269:31807–13. [PubMed: 7527397]

Mattoon DR, Lamothe B, Lax I, Schlessinger J. The docking protein Gab1 is the primary mediator of EGF-stimulated activation of the PI-3K/Akt cell survival pathway. BMC Biol. 2004; 2:24. [PubMed: 15550174]

Miranti CK, Brugge JS. Sensing the environment: a historical perspective on integrin signal transduction. Nat Cell Biol. 2002; 4:E83–90. [PubMed: 11944041]

Moro L, Dolce L, Cabodi S, Bergatto E, Erba EB, Smeriglio M, et al. Integrin-induced epidermal growth factor (EGF) receptor activation requires c-Src and p130Cas and leads to phosphorylation of specific EGF receptor tyrosines. J Biol Chem. 2002; 277:9405–14. [PubMed: 11756413]

Nurmenniemi S, Sinikumpu T, Alahuhta I, Salo S, Sutinen M, Santala M, et al. A Novel Organotypic Model Mimics the Tumor Microenvironment. Am J Pathol. 2009

Onishi A, Chen Q, Humtsoe JO, Kramer RH. STAT3 signaling is induced by intercellular adhesion in squamous cell carcinoma cells. Exp Cell Res. 2008; 314:377–86. [PubMed: 17961551]

Pece S, Gutkind JS. Signaling from E-cadherins to the MAPK pathway by the recruitment and activation of epidermal growth factor receptors upon cell-cell contact formation. J Biol Chem. 2000; 275:41227–33. [PubMed: 10969083]

Pore N, Jiang Z, Gupta A, Cerniglia G, Kao GD, Maity A. EGFR tyrosine kinase inhibitors decrease VEGF expression by both hypoxia-inducible factor (HIF)-1-independent and HIF-1-dependent mechanisms. Cancer Res. 2006; 66:3197–204. [PubMed: 16540671]

Ranganathan AC, Adam AP, Aguirre-Ghiso JA. Opposing roles of mitogenic and stress signaling pathways in the induction of cancer dormancy. Cell Cycle. 2006; 5:1799–807. [PubMed: 16929185]

Rodrigues GA, Falasca M, Zhang Z, Ong SH, Schlessinger J. A novel positive feedback loop mediated by the docking protein Gab1 and phosphatidylinositol 3-kinase in epidermal growth factor receptor signaling. Mol Cell Biol. 2000; 20:1448–59. [PubMed: 10648629]

Santini MT, Rainaldi G, Indovina PL. Apoptosis, cell adhesion and the extracellular matrix in the three-dimensional growth of multicellular tumor spheroids. Crit Rev Oncol Hematol. 2000; 36:75–87. [PubMed: 11033298]

Schmidt MH, Furnari FB, Cavenee WK, Bogler O. Epidermal growth factor receptor signaling intensity determines intracellular protein interactions, ubiquitination, and internalization. Proc Natl Acad Sci U S A. 2003; 100:6505–10. [PubMed: 12734385]

Schneider MR, Wolf E. The epidermal growth factor receptor ligands at a glance. J Cell Physiol. 2009; 218:460–6. [PubMed: 19006176]

Shen X, Kramer RH. Adhesion-mediated squamous cell carcinoma survival through ligand-independent activation of epidermal growth factor receptor. Am J Pathol. 2004; 165:1315–29. [PubMed: 15466396]

Singh AB, Harris RC. Autocrine, paracrine and juxtacrine signaling by EGFR ligands. Cell Signal. 2005; 17:1183–93. [PubMed: 15982853]

Singh AB, Sugimoto K, Harris RC. Juxtacrine activation of epidermal growth factor (EGF) receptor by membrane-anchored heparin-binding EGF-like growth factor protects epithelial cells from anoikis while maintaining an epithelial phenotype. J Biol Chem. 2007; 282:32890–901. [PubMed: 17848576]

Thelemann A, Petti F, Griffin G, Iwata K, Hunt T, Settinari T, et al. Phosphotyrosine signaling networks in epidermal growth factor receptor overexpressing squamous carcinoma cells. Mol Cell Proteomics. 2005; 4:356–76. [PubMed: 15657067]

Walker JL, Assoian RK. Integrin-dependent signal transduction regulating cyclin D1 expression and G1 phase cell cycle progression. Cancer Metastasis Rev. 2005; 24:383–93. [PubMed: 16258726]

Weidner KM, Di Cesare S, Sachs M, Brinkmann V, Behrens J, Birchmeier W. Interaction between Gab1 and the c-Met receptor tyrosine kinase is responsible for epithelial morphogenesis. Nature. 1996; 384:173–6. [PubMed: 8906793]
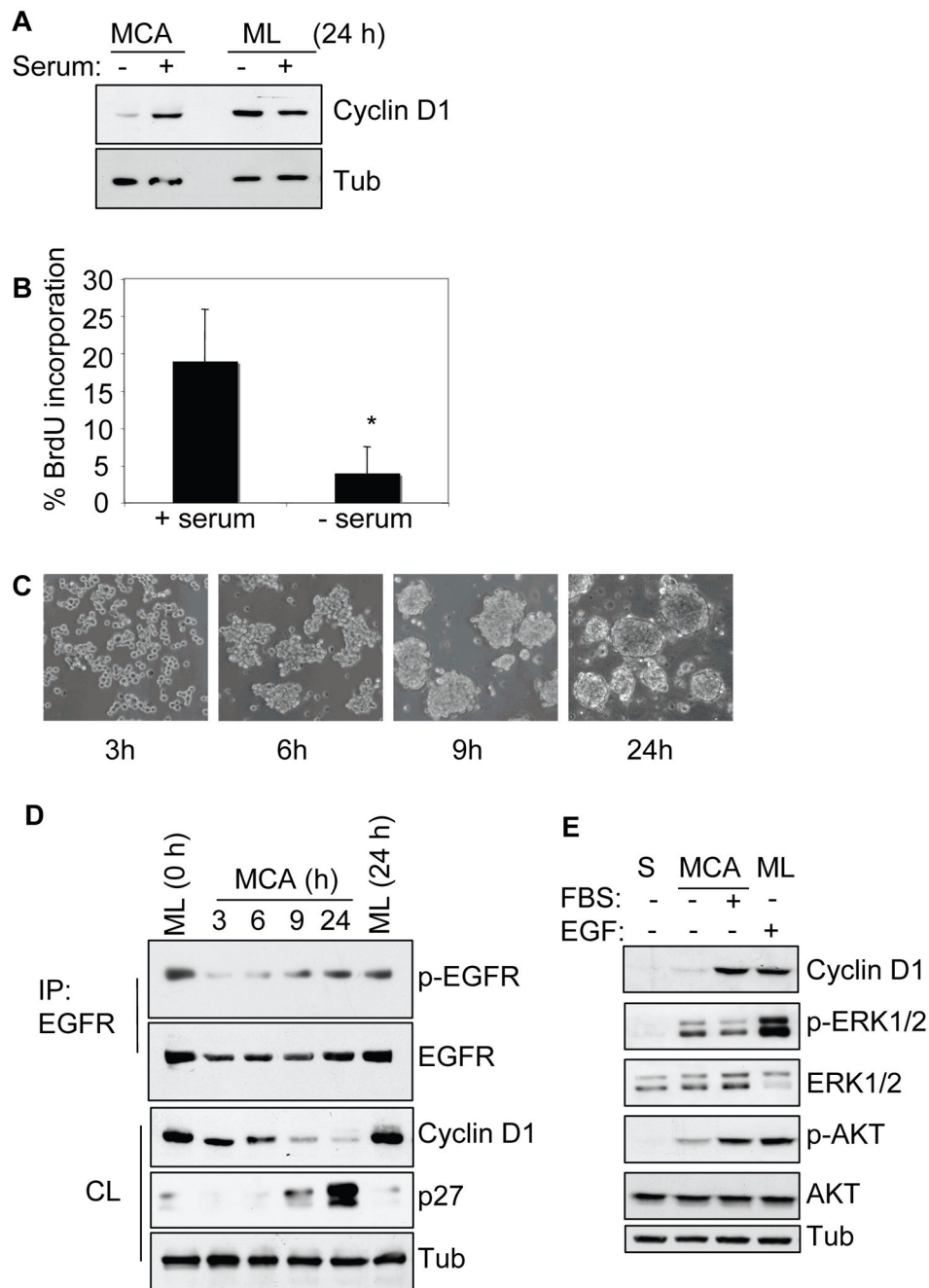
Figure 1.
Serum-deprivation suppresses cyclin D1 expression and proliferation in MCA (A) HSC-3 cells as monolayer (ML) or MCA cultured for 24 h, with or without 10% serum were lysed and analyzed by immunoblotting for cyclin D1 expression. (B) Cells subjected to MCA formation as above were assessed for BrdU uptake as described in Materials and Methods and represented as % BrdU incorporation (mean±SD, * $p < 0.05$). (C) Photomicrograph of HSC-3 MCAs showing the aggregate formation and compactness with time in serum-free DMEM culture. D) MCAs as in (C) were collected, lysed and analyzed for cyclin D1 and

p27 expression or immunoprecipitated (IP) and analyzed for phospho-EGFR and total EGFR. Serum-starved ML cells at 0 h (time MCA started) and 24 h (time final MCA collected) were included as controls. (E) HSC-3 cells were subjected to single cell suspension (S) or as MCA in the absence or presence of serum. After 24 h, cells were collected, lysed, and processed for immunoblotting as indicated. Membranes were stripped and reprobed for total ERK1/2 and AKT. Cell lysates from serum-starved ML culture treated with EGF (10 ng/ml) for 5 min, were included as a control for ERK and AKT activation. Tubulin was used as loading control wherever indicated. The results are representatives of at least three independent experiments.
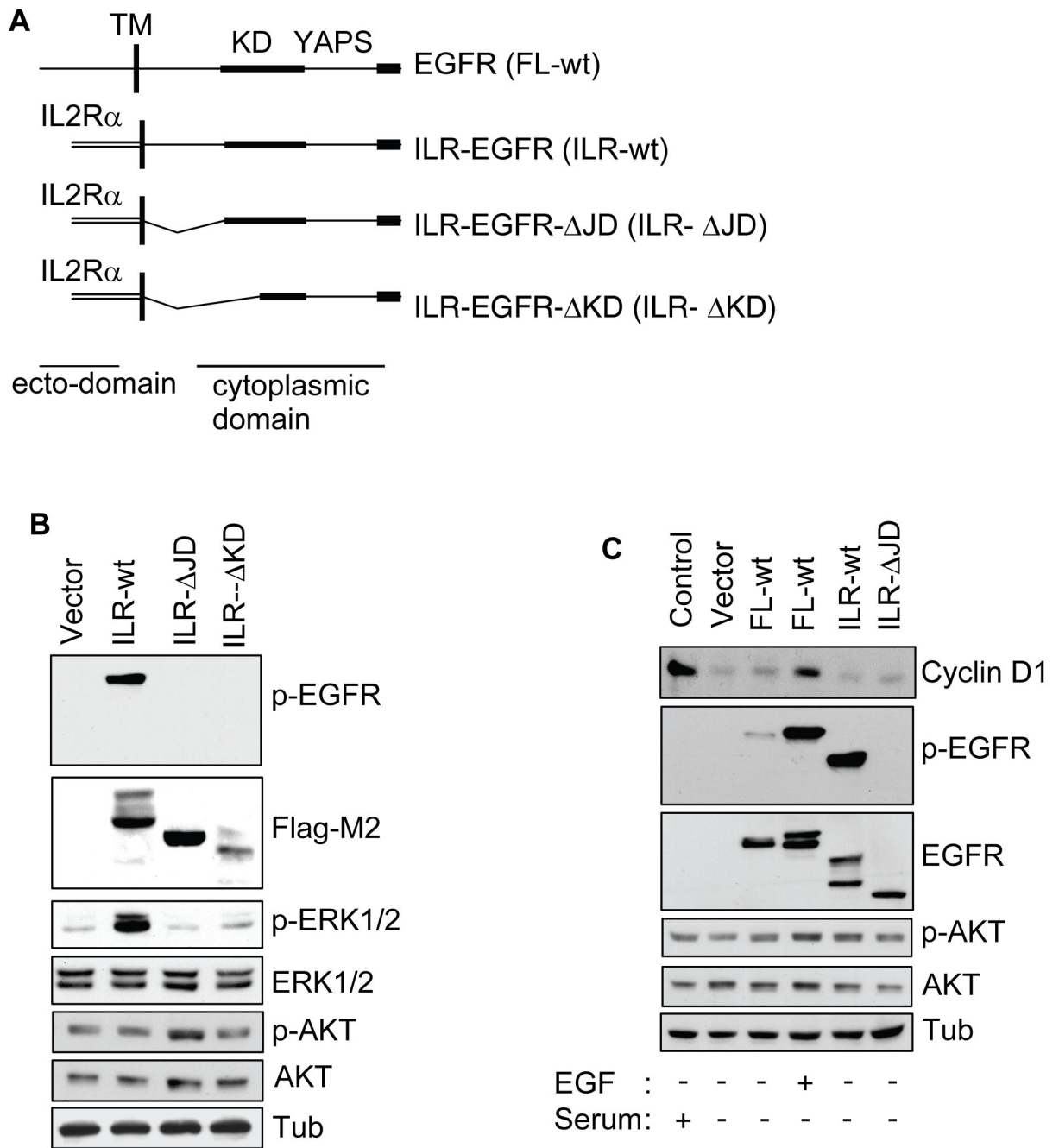
Figure 2.
Ligand-independent EGFR activation is not sufficient for induction of cyclin D1 and
proliferation. (A) Schematic representation of C-terminal Flag-tagged EGFR and
interleukin-2 receptor (ILR)-EGFR-chimera constructs. The ILR-wt contains ILR
ectodomain fused to the EGFR cytoplasmic region; ILR- JD contains ILR ectodomain and
EGFR cytoplasmic region lacking 33 amino acids at the juxtadomain and ILR- KD contains
ILR ectodomain and the EGFR cytoplasmic region lacking juxtadomain and a segment of
the kinase domain. TM, transmembrane; KD, kinase domain; YAPS, tyrosine

autophosphorylation sites. (B) Protein lysates from HEK293 cells transfected with the various constructs were immunoblotted as indicated. (C) HEK293 cells transiently expressing the indicated constructs were cultured in the absence of serum for 18 h and with or without EGF (10 ng/ml). Protein lysates were then prepared and analyzed by immunoblotting as indicated. The phospho-EGFR and p-AKT membranes were stripped and reprobed with anti-EGFR and AKT antibody, respectively. Note that the p-AKT level in presence of serum and EGF are not prominent compared to the others. This is likely due to global endogenous AKT activity emancipating from the adherent cells. The results are representative of 2 independent experiments.
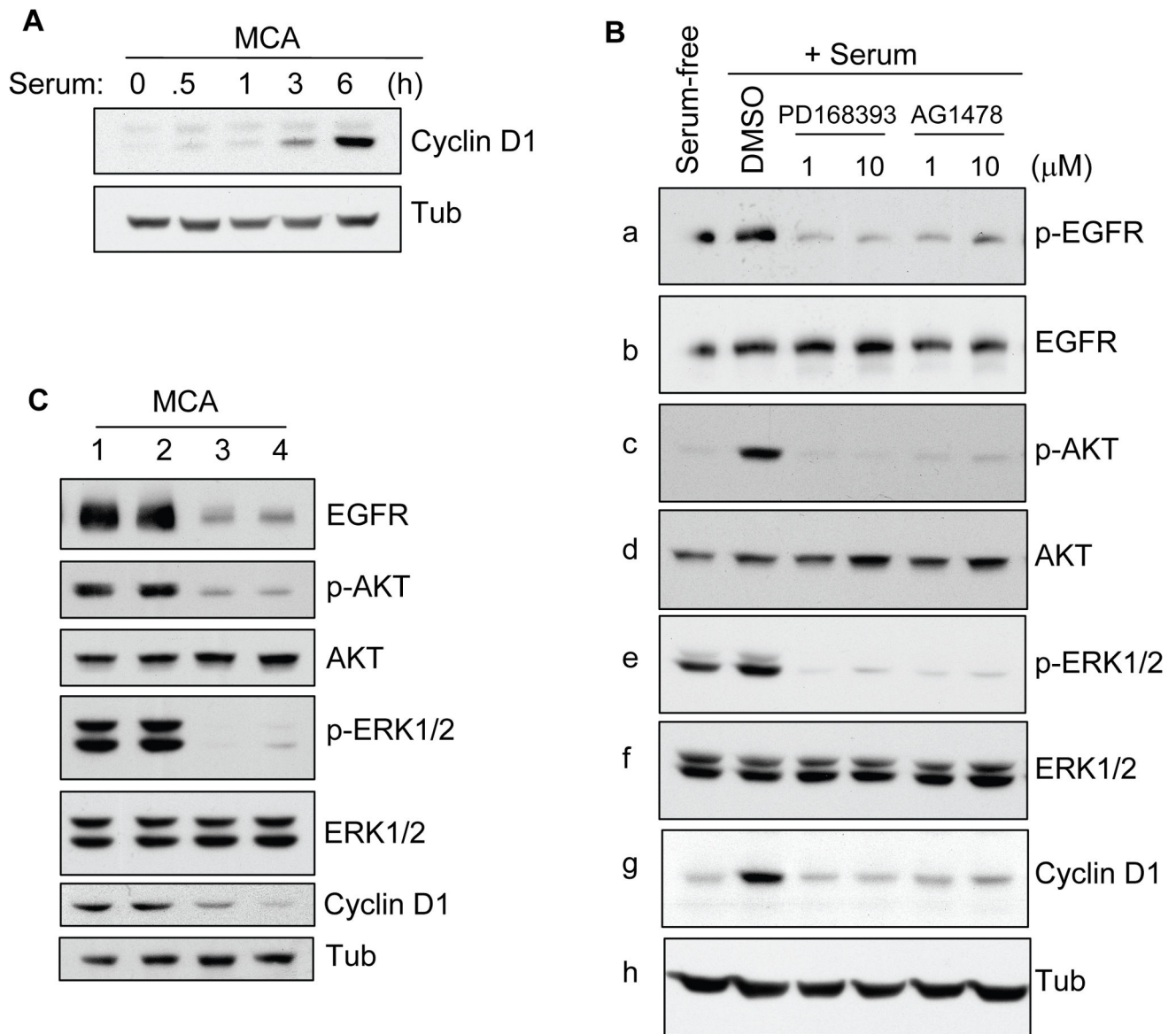
Figure 3.
Effects of EGFR signaling on serum-dependent cyclin D1 expression in MCAs. (A) HSC-3 cells were subjected to MCA formation without serum. After 20 h, aggregates (pre-formed MCA) were obtained by brief centrifugation (1000 rpm, 2 min) and incubated in 10% FBS containing DMEM in pre-coated poly-HEMA dishes. MCAs were collected at various time points as indicated, lysed, and processed for immunoblotting for cyclin D1. (B) Pre-formed MCAs as above were incubated with serum in the presence of DMSO alone, and 1 or 10 μM of PD168393 and AG1478 for 6 h. Cell lysates were prepared and immunoblotted for cyclin D1, p-EGFR, p-AKT and p-ERK1/2. Each membrane was stripped and reprobed for its corresponding total protein as indicated. Tubulin was used as an additional control protein loading. Results are representative of 2 independent experiments. (C) HSC-3 cells transfected with siRNA against EGFR were subjected to MCAs formation in presence of 10% FBS for 24 hr. Cell lysates were prepared and analyzed by Western blotting as

indicated. Lane 1 is untransfected control; lane 2 is transfected with control-scrambled siRNA; lane 3 is transfected with 25 nM and lane 3 is with 100 nM EGFR-siRNA, respectively.
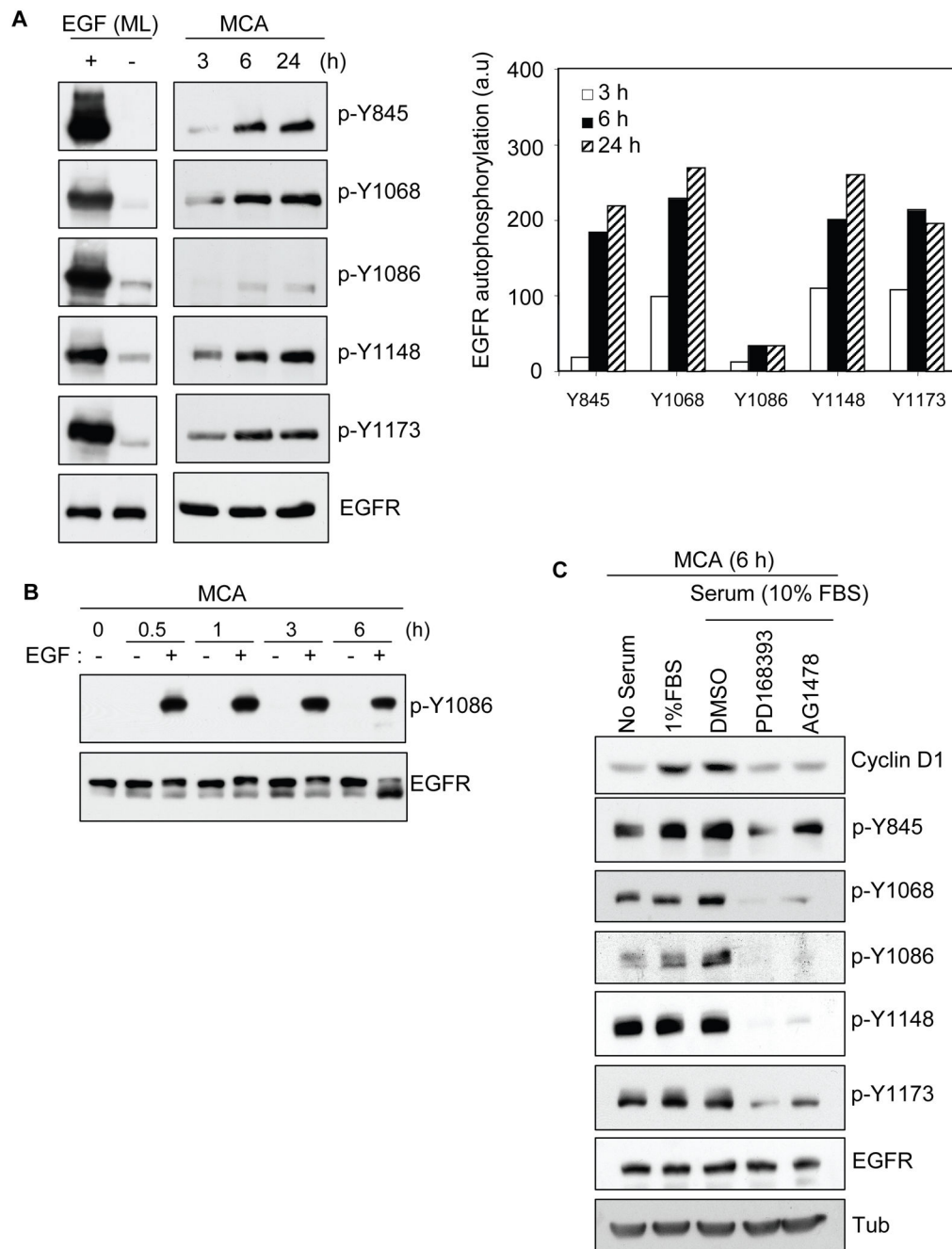
Figure 4.
Inefficient EGFR autophosphorylation in serum-deprived MCA is associated with cyclin D1 expression. (A) Serum-starved HSC-3 cells were detached and incubated on poly-HEMA coated dishes in DMEM without serum. Cells at varying levels of aggregation were collected, lysed, and analyzed with various phospho-specific EGFR antibodies and total EGFR as indicated (right panel: densitometry analysis of the phosphorylated tyrosine residues represented in arbitrary units). Samples from serum-starved monolayer cells, treated with or without EGF (10 ng/ml) for 15 min, are included as positive references for the different phospho-EGFR antibodies used. (B) Pre-formed MCAs were incubated in

DMEM alone and with or without EGF (10 ng/ml). After different time durations, MCAs were collected, lysed, and immunoblotted with p-Y1086 antibody. The membrane was stripped and re-blotted for total EGFR. (C) Pre-formed MCAs as in Figure 3 were incubated in DMEM containing no serum or with 1 or 10% FBS. PD168393 and AG1478 (EGFR inhibitors) were included at 1 μM to MCAs supplemented with 10% FBS. After 6 h, MCAs were collected, lysed, and processed for immunoblotting as indicated. A representative membrane was stripped and reprobed with anti-EGFR. Tubulin was monitored for equivalent protein load. Representative result from three independent experiments is shown.
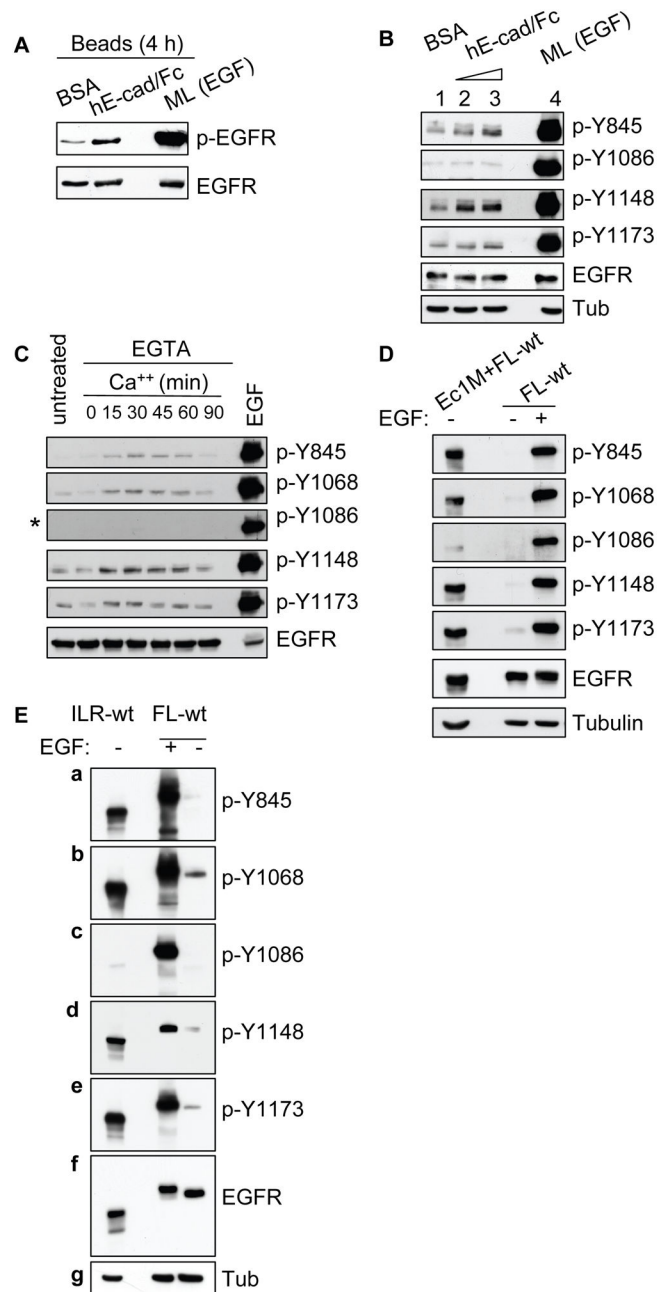
Figure 5.
Analysis of differential EGFR autophosphorylation mediated by a ligand-independent
mechanism. (A) HSC-3 cells were detached and incubated in DMEM on poly-HEMA plates
in the presence of beads coated with BSA or hE-Cad/Fc (about 0.25×10^6 beads/1×10^6
cells). Cells were collected after 4 h and processed for phospho-EGFR activity by Western
blot. The membrane was stripped and reprobed for total EGFR. (B) Cells as above were
incubated with BSA-coated beads (lane 1) and two varying concentrations (0.1×10^6
beads/1×10^6 cells, and 0.5×10^6/1×10^6 cells) of hE-Cad/Fc coated beads (lane 2 and 3,
respectively). After 4 h, cells were collected, lysed and analyzed by immunoblotting as

indicated. (C) Calcium switch assay: HSC-3 cells subjected to Ca^{++} switch assay were collected at varying time points and analyzed with different phospho-specific EGFR antibodies. Cells left untreated with Ca^{++} or cells stimulated with EGF for 15 min were included as controls. Asterix (*) indicates the prolonged x-ray film exposure. (D) FL-wt and Ec1M (Chitaev and Troyanovsky, 1998) co-expressing HEK293 cells, or FL-wt expressing cells alone (stimulated with or without EGF) were non-enzymatically detached and cultured in serum-free medium for 30 min. Cell lysates were prepared and analyzed by Western blotting. (E) HEK293 cells expressing ILR-wt or FL-wt treated with or without EGF (10 ng/ml) for 15 min, were lysed and analyzed by immunoblotting as indicated (a-e). Membranes were stripped and reprobed with EGFR and tubulin antibody as loading controls. Results are representative of 2–4 independent experiments.
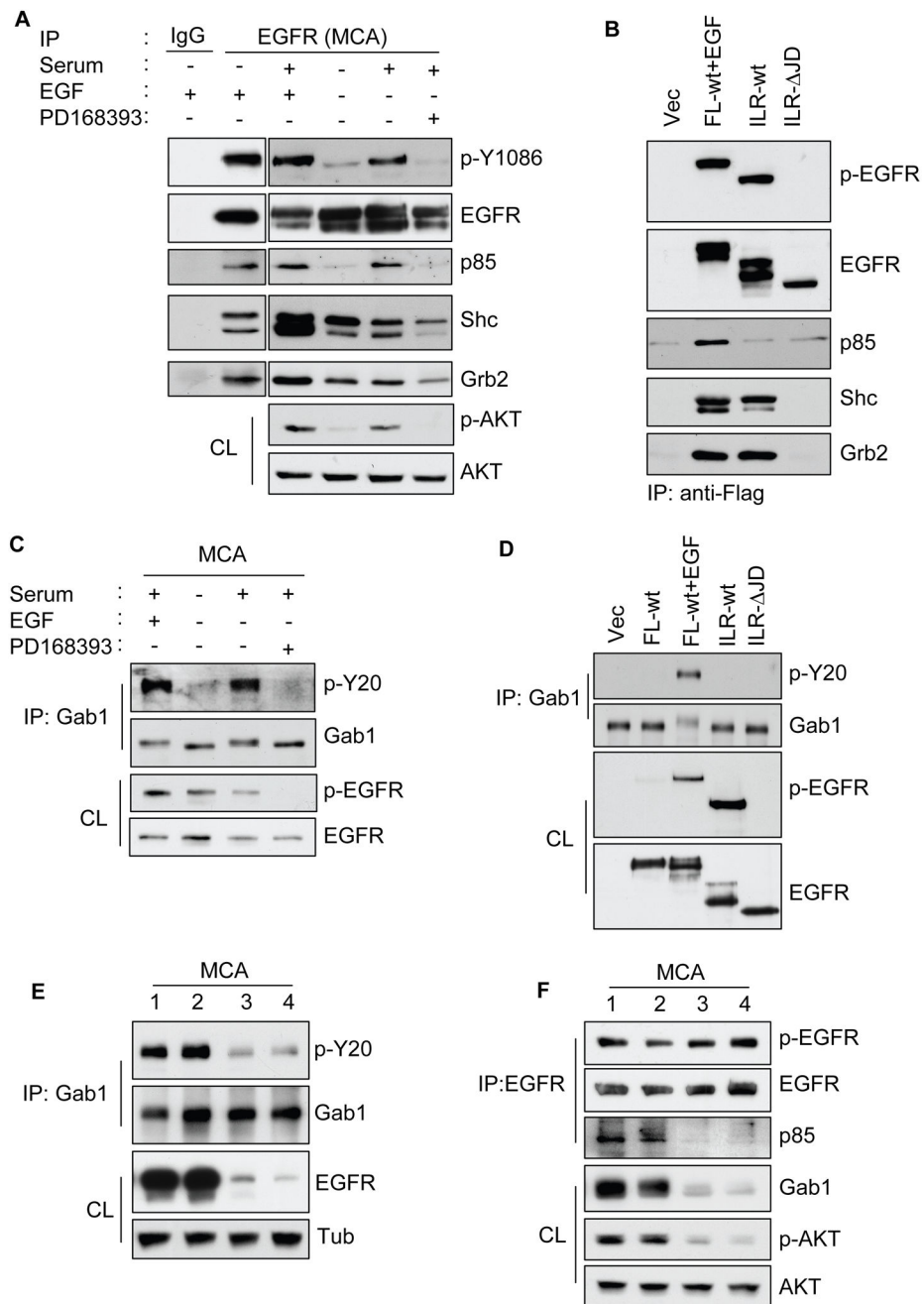
Figure 6.
Ligand-independent EGFR activation is unable to recruit the Gab-1/p85/AKT signaling complex. (A) Pre-formed MCAs as in Figure 3 were incubated in DMEM containing either no serum or 10% FBS containing either EGF (10 ng/ml) or 1 μM PD168393. After 6 h, MCAs were collected and lysed, and about 250 μg of protein from each condition were used for immunoprecipitation (IP) with 2 μg control mouse IgG or anti-EGFR. The IP was then analyzed by immunoblotting as indicated. Cell lysates (CL) were analyzed with anti-p-AKT (stripped and reprobed with anti-AKT). (B) HEK293 cells expressing the various indicated constructs were lysed and IP with anti-Flag. The IP was then analyzed by immunoblotting as

indicated. FL-wt expressing cells were stimulated with EGF (10 ng/ml) for 10 min (C) Pre-formed HSC-3 MCAs incubated as in (A) were lysed, IP with anti-Gab1 and then analyzed with anti-pY20 (phosphotyrosine). The membrane was stripped and reprobed for total Gab-1. CL was also analyzed for the phospho-EGFR status. (D) HEK293 cells expressing the various constructs as indicated were lysed and IP with anti-Gab1 and analyzed with anti-pY20. The membrane was stripped and reprobed for total Gab1. CL was also analyzed for phospho-EGFR or total EGFR to confirm expression of the constructs. FL-wt expressing cells were stimulated with EGF (10 ng/ml) for 10 min. (E) EGFR-siRNA transfected HSC-3 cells were subjected to MCAs formation in presence of 10% FBS for 24 hr. Cell lysates were prepared and analyzed by IP and Western blotting as indicated. (F) Gab1-siRNA transfected HSC-3 cells were subjected to MCAs formation as above. Cell lysates were prepared and analyzed by IP and Western blotting as indicated. In (E) and (F), lanes 1 are untransfected control; lanes 2 are transfected with control-scrambled siRNA; lanes 3 are transfected with 25 nM and lanes 4 are with 100 nM of either EGFR- or Gab1-siRNA, respectively. Results are representative of at least 2–4 independent experiments.
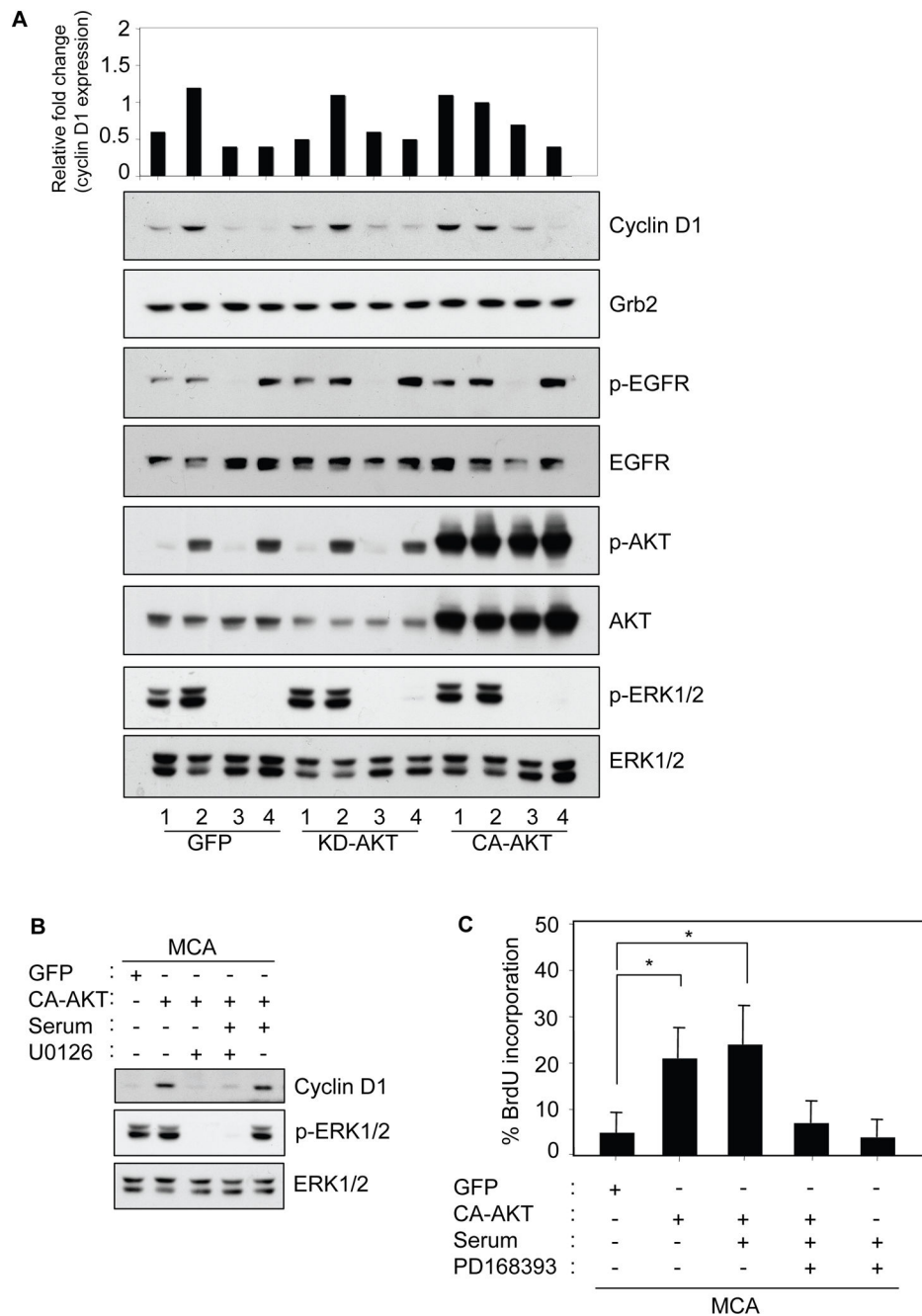
Figure 7.
Constitutively active AKT establishes cyclin D1 expression and proliferation in MCA without serum in an EGFR-dependent manner. (A) Monolayer HSC-3 cells were infected with adenovirus for GFP, KD-AKT (GFP-tagged kinase dead AKT), and CA-AKT (GFP-tagged constitutively active AKT) for 18 h. Cells were detached and subjected to MCA formation in DMEM either with or without serum (10% FBS). After 24 h, MCAs were collected, lysed, and analyzed by immunoblotting as indicated. Grb2 was used as an internal loading control. The top panel represents relative fold change of cyclin D1 as measured by NIH Image. Lanes 1, MCA with no serum; lanes 2, MCA with serum; lanes 3, MCA with

serum treated with 1 μM PD168393; and lanes 4, MCA with serum and treated with 1 μM U0126. (B) GFP and CA-AKT expressing MCAs as in (A) and treated with 10 μM U0126 was lysed and analyzed by immunoblotting as indicated (C) GFP and CA-AKT expressing MCA were cultured in the presence of 50 μM BrdU with or without serum for 24 h. MCAs were then collected, trypsinized, washed, and allowed to attach on poly-lysine coated coverslips for anti-BrdU immunostaining. The total cell number and BrdU positive cells from 5–10 random microscopic fields comprising from 3–5 sample slides (* $p < 0.05$) were counted and represented as % BrdU incorporation (mean±SD). Results are representative of two independent experiments.